ACS NANO
Cite This: ACS Nano 2018, 12, 1491−1499
www.acsnano.org
ARTICLE

Self-Powered Microfluidic Transport System Based on Triboelectric Nanogenerator and Electrowetting Technique

Jinhui Nie,[†,‡] Zewei Ren,[†,‡] Jiajia Shao,[†,‡] Chaoran Deng,[†,‡] Liang Xu,[†,‡] Xiangyu Chen,[*,†,‡] Meicheng Li,[*,§] and Zhong Lin Wang[*,†,‡,∥]

[†]Beijing Institute of Nanoenergy and Nanosystems, Chinese Academy of Sciences, Beijing 100083, P. R. China
[‡]School of Nanoscience and Technology, University of Chinese Academy of Sciences, Beijing 100049, P. R. China
[§]State Key Laboratory of Alternate Electrical Power System with Renewable Energy Sources, School of Renewable Energy, North China Electric Power University, Beijing 102206, P. R. China
[∥]School of Material Science and Engineering, Georgia Institute of Technology, Atlanta, Georgia 30332-0245, United States

Supporting Information

ABSTRACT: **Electrowetting technique is an actuation method for manipulating position and velocity of fluids in the microchannels. By combining electrowetting technique and a free-standing mode triboelectric nanogenerator (TENG), we have designed a self-powered microfluidic transport system. In this system, a mini vehicle is fabricated by using four droplets to carry a pallet (6 mm × 8 mm), and it can transport some tiny object on the track electrodes under the drive of TENG. The motion of TENG can provide both driving power and control signal for the mini vehicle. The maximum load for this mini vehicle is 500 mg, and its highest controllable velocity can reach 1 m/s. Free-standing TENG has shown excellent capability to manipulate microfluid. Under the drive of TENG, the minimum volume of the droplet can reach 70−80 nL, while the tiny droplet can freely move on both horizontal and vertical planes. Finally, another strategy for delivering nanoparticles to the designated position has also been demonstrated. This proposed self-powered transport technique may have great applications in the field of microsolid/liquid manipulators, drug delivery systems, microrobotics, and human-machine interactions.**

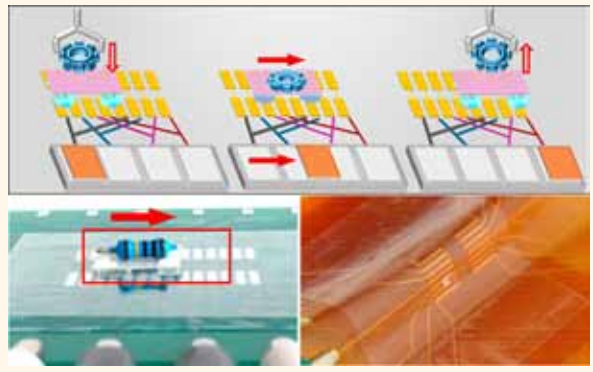

KEYWORDS: *triboelectric nanogenerator, electrowetting technique, microfluid, liquid robotics, self-powered system*

Microfluidics is related to the precise control and manipulation of fluids with small volumes, and it is the essential element for many applications, including biochemical analysis, adaptive lens, drug delivery, printing techniques, and so on.[1−4] In order to achieve the effective control of position and velocity of fluids in the microchannels, it is quite necessary to develop some actuation methods that can operate locally on the fluids.[5] One of these methods is electrowetting technique,[4] which can manipulate contact angle of the liquid droplets by applying electric fields. Electrowetting has several extremely attractive advantages, such as low energy consumption, fast response speed and scalability, which is good for the system in micrometer scale.[4,6] However, in the real application of electrowetting, a dielectric film is usually employed to separate fluids from electrodes, which leads to high switching voltages. In most studies, it needs at least 200 V to obtain a significant change of contact angle. This high voltage applied for microfluidics is usually provided by a power source, where a sophisticated control circuit is also prepared to regulate the motion distance and velocity of the microfluids. The high voltage source and the control circuits increase the complexity of the microfluidic system, which can be a hurdle for expanding the application of this technique. Accordingly, all these facts inspired us to develop a fully self-powered microfluidic system, where both the power source and the control circuits can be spared.

In the past few years, triboelectric nanogenerator (TENG), which can directly convert quite a lot of mechanical energy in our daily activity into electricity, has been employed as the energy supplier for many electronic and electromechanical systems.[7−11] The output characteristic of the TENG is a high

Received: November 12, 2017
Accepted: January 17, 2018
Published: January 17, 2018

DOI: 10.1021/acsnano.7b08014
ACS Nano 2018, 12, 1491−1499

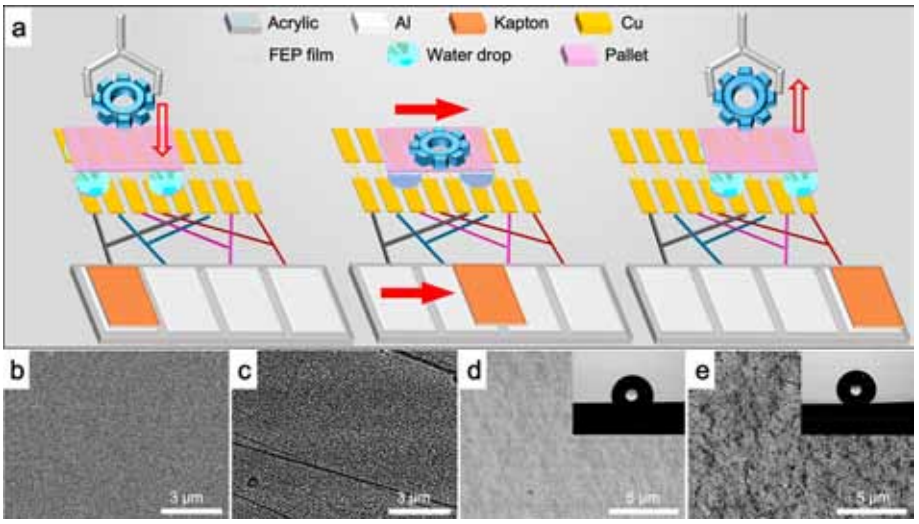

Figure 1. Schematic illustration of the self-powered microfluidic transport system. (a) Structure of the self-powered microfluidic transport system based on TENG and electrowetting technique to control the mini vehicle carrying a tiny gear. (b, c) SEM image of the Kapton film before and after ICP treatment. (d, e) SEM image of the FEP film before and after hydrophobic treatment. Insets: The contact angle of FEP film.

output voltage and a low output current. The short-circuit current is usually at the scale of milliampere or microampere, while the open-circuit voltage can reach a few thousands volts.[12−16] Accordingly, by utilizing its voltage signal, the TENG can effectively drive or control some smart electromechanical systems, and various interesting applications in the field of tunable optical devices,[17,18] soft robotics[19,20] and wearable electronics[21,22] have been realized. Here, TENG can provide both driving power and control signal for various electromechanical systems, and it can work as a bridge for realizing human-machine interactions. Therefore, TENG can also be smoothly combined with electrowetting technique to realize a self-powered manipulation of microfluids. The fast response capability of TENG can ensure an effective operation of microfluids, while the good insulating performance of electrowetting system can fully preserve the tribo-induced electrostatic field. The combination of these two techniques can open up a variety of potential applications for TENG-based self-powered technique.

In this study, in order to demonstrate the control ability of TENG-based microfluidic system, a mini vehicle with four droplets as the wheels is fabricated and combined with the TENG driving system. The size of mini vehicle is in the millimeter scale, and it can carry some tiny objects to realize a microtransport system. A freestanding mode TENG with grid electrodes is designed to precisely control the stepping motion of microfluids. The freestanding structure can achieve a very small internal capacitance, and the multiple grid electrodes can increase the tribo-induced charges. Accordingly, the driving capability of this self-powered microfluidic system is strongly enhanced, and the minimum volume of the droplet can reach tens of nanoliters, which is over 250 times smaller than the previous study.[20] The sliding motions can serve as the driving power for the system, and the microfluid can move synchronously with the TENG. Thus, no power source or control circuits are needed in this system. This study may have great potential applications in the field of electrowetting technique, microfluid manipulation, human-robotic interaction, and so on.

RESULTS AND DISCUSSION

The structure of the integrated self-powered microfluidic transport system based on TENG and electrowetting technique is shown in Figure 1a. The pallet for carrying some tiny objects is sustained by four droplets, which can form a mini vehicle device. The droplets lay on the hydrophobic surface, and two lines of grating track electrodes are placed beneath the hydrophobic film to guide the motion of the droplets. The output voltage from TENG is applied on the track electrodes, and the droplets can be moved by the generated Coulomb force, which is related to electrowetting phenomenon. Hence, a mini vehicle device can be established, and the motion of this mini vehicle can be driven and controlled by the TENG. The freestanding mode TENG with grid electrodes is the core element of the system, whereas the output voltage is generated by tribo-electrification happening between Kapton film and four pieces of Al foil. In order to increase the tribo-induced charge density and further enhance the output performance of TENG, inductively coupled plasma (ICP) treatment is applied on the surface of the Kapton film.[19,20] Hence, the Kapton film is covered with a series of nanopatterned structures, and the related scanning electron microscopy (SEM) images can be found in Figure 1b (before ICP treatment) and Figure 1c (after ICP treatment). The output voltage generated by the electrification between Kapton film and Al foil is the driving power for the system, and the sliding motion of the TENG can precisely control the movement of the mini vehicle. The detailed mechanism about the motion of the droplet under the drive of TENG will be explained later. The structure of the mini vehicle and the composition of hydrophobic substrate can be found in Figure S1 in the Supporting Information. The pallet in the mini vehicle is fabricated by a polystyrene substrate covered by polyvinylidene fluoride (PVDF) film, and the PVDF side is contacted four droplets. Two lines of track electrodes made of Cu are periodically printed on the surface of insulating substrate, and a polytetrafluoroethylene (PTFE) film is attached on top of grating electrodes, in order to prevent breakdown phenomenon between adjacent electrodes (see Figure S1). Even if the gap between two electrodes was

DOI: 10.1021/acsnano.7b08014
ACS Nano 2018, 12, 1491−1499

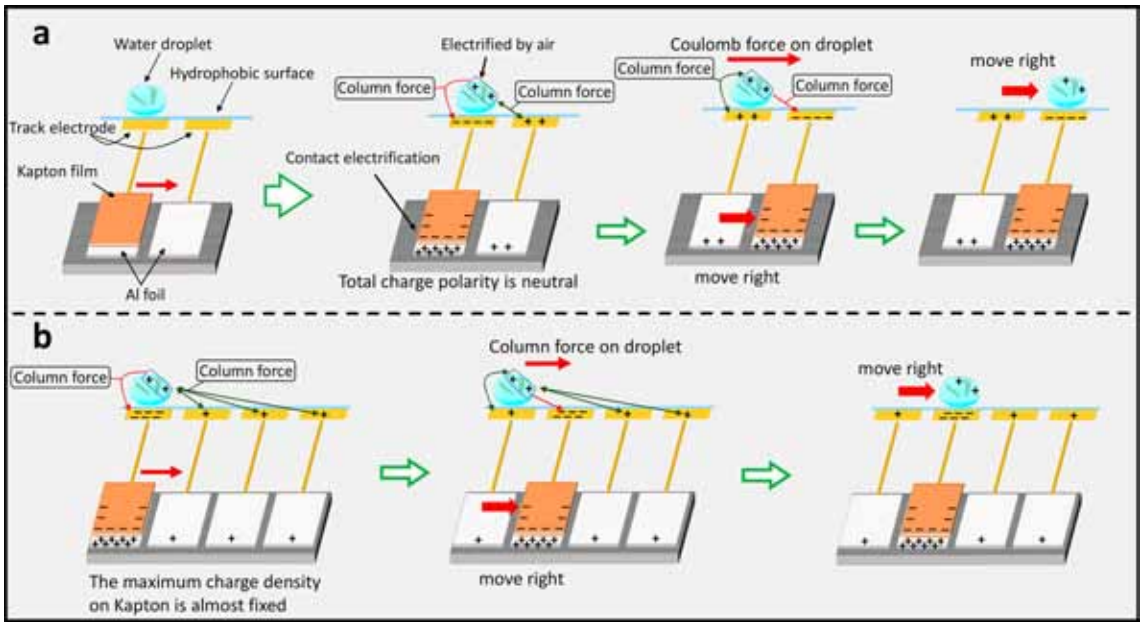

Figure 2. Working principle of the self-powered microfluidic transport system. (a) The working principle of the system with two electrodes. (b) The working principle of the system with four electrodes.

decreased to 0.5 mm, the system can still work stably. Then, a fluorinated ethylene propylene (FEP) film is attached on top of PTFE, and the droplets of the mini vehicle move on the surface of FEP film. The surface of FEP film is naturally hydrophobic. However, in order to further increase the hydrophobicity, we applied chemical treatment on FEP film. The SEM images of the FEP surface are shown in Figure 1d (before hydrophobic treatment) and Figure 1e (after hydrophobic treatment). The inset photos in Figure 1d,e give the change of contact angle before (105°) and after hydrophobic treatment (145°). The hydrophobic surface will ensure the water droplet to move smoothly on the surface of FEP, which effectively enhances the performance of the actuation.

The detailed working mechanism of this freestanding mode TENG and the whole microtransport system is illustrated in Figure 2a,b. For the simple case, we will first consider the two electrodes TENG device, as can be seen in Figure 2a. The contact electrification results in the negative charges on the Kapton film, and the amount of the negative charges on Kapton film is equal to the total positive charges on two Al foils, which is the basic working principle of freestanding mode TENG.[16] Each Al foil is connected with a track electrode on the hydrophobic substrate, and the water droplet is placed on top of the hydrophobic substrate. The water droplet is positively electrified during the friction motion with air, as can be seen in Figure 2a. When Kapton film is overlapped the left foil, the excessive negative charges on the Kapton film cannot be fully neutralized by the positive charges on the Al foil. Hence, the negative charges are induced on the related track electrode, and the droplet is attracted to the left electrode due to Coulomb force, as illustrated in Figure 2a. Then, Kapton film is slid to the right foil, and the induced charges on two track electrodes are switched (see Figure 2a). Accordingly, the positive charges on the left electrode provide a pushing force to the droplet, while the negative charges on the right electrode generate a pulling force to the droplet. The water droplet moves to the right electrode under the drive of Coulomb force, and this is the basic operation mechanism of this self-powered microfluidic system. The microfluidic system with multiple track electrodes is illustrated in Figure 2b. It is important to note that the tribo-induced charges on Kapton film has a maximum value. As can be seen in Figure 2b, the negative charges are induced on the Kapton film, and the same amount of positive charges is shared by all the four Al foils. This mechanism illustration is related to the steady operation state, which is based on the real measurement (see the later part). In order to simplify the understanding, we assume that positive charges are equally distributed on four foils, as can be seen in Figure 2b. The basic operation mechanism for this four electrodes' device is similar to the double electrodes' case. The Al foil overlapped by Kapton film will be negatively electrified, which is due to the massive negative charges on Kapton surface. When the electrostatic field between two electrodes is established, Coulomb force will be applied on the positively charged droplet. Then, the droplet moves away from the positively charged electrode and moves close to the negatively charged electrode. Based on this mechanism, the water droplet can move synchronously with the Kapton film on the track electrodes. The mechanical motion of TENG can work as both the power supplier and the controlling signal to lead the step motion of droplet. The strength of this Coulomb force is determined by the generated tribo-charges from TENG and the gap distance between two electrodes. The multi-electrodes structure allowed each electrode to share less positive charges, and thus negatively charged Kapton film can induce more negative charges on the related track electrode, as can be seen in Figure 2a,b. Meanwhile, the surface modification process has been applied to Kapton surface, which can increase the saturated charge density on Kapton surface. Hence, this freestanding mode TENG with grating electrodes can effectively regulate the motion of the droplet in the microfluidic system. Based on this working principle for manipulating a single droplet, the mini vehicle with four droplets as the wheels can also be driven and controlled by TENG. As can be seen in Figure 1a, four groups of track electrodes are prepared for each water droplet in the mini vehicle, and each Al foil in the

DOI: 10.1021/acsnano.7b08014
ACS Nano 2018, 12, 1491−1499

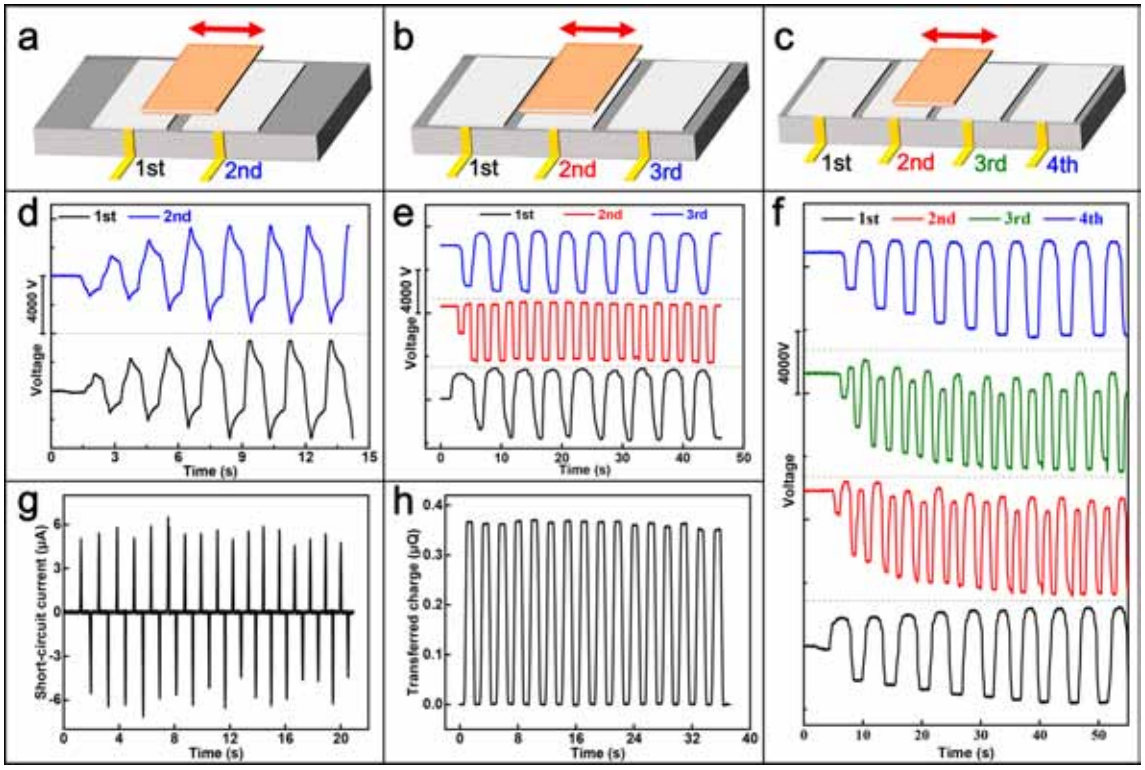

Figure 3. Electrical output performances of TENG with three different numbers of Al foils. (a–c) The illustration of the free-standing TENG with two, three, and four electrodes, respectively. (d–f) Open-circuit voltage of the single electrode of the free-standing TENG with two, three, and four electrodes, respectively. (g) Short-circuit current and (h) transferred charge of the single-electrode TENG. (The tribo-surface between Kapton and Al foil is 8 cm × 10 cm.)

freestanding TENG is simultaneously connected to four track electrodes that belonged to four different electrode groups. In this case, the output signal from TENG can simultaneously control the motion of four droplets. Accordingly, when the Kapton film slides from one side to the other, the mini vehicle is driven to the other side synchronously, and thus a microtransport system can be established.

To predict the generated electric field by the TENG, the potential distribution of the electrodes is calculated by a finite element method (FEM) in the COMSOL software, as shown in Figure S2a–c. In the FEM model, the electric field and driving force can be analyzed based on the simulation, and the summarized data about the generated electrostatic force on horizontal direction can be seen in Figure S2d. Specifically, the left electrode has a positive voltage (3000 V), and the right electrode has a negative voltage (−3000 V). At the first state, the droplet with positive charges is subject to a large horizontal electrostatic repulsion due to the applied potential on the left electrode, as shown in Figure S2a. At this moment, the droplet starts to move with a big acceleration. When the droplet reaches the middle region of the two electrodes, the decrease of electric field leads to the decrease of driving force (see Figure S2b), and the acceleration of the droplet decreases. Finally, when the droplet approaches the right electrode, the attractive force from the right electrode increases, and the acceleration of the droplet rises again. The acceleration of the droplet is decided by the applied driving force and the friction force between droplet and FEP surface, while the friction force of the droplet is related to the contact angle of the droplet. For the relationship between contact angle and the sliding friction of the droplet, a series of studies has been done by other researchers.[23,24] Generally speaking, the interaction energy between water and substrate is proportional to the true contact area. Thus, the increase of the contact angle decreases the contact area, and the friction force of the droplet on the FEP film also decreases accordingly. As can be seen in Figure S2d, the driving force on the horizontal direction has two peaks on both left and right edges, while the driving force decreased significantly in the middle region. This phenomenon decides that the droplet has a maximum driving distance. If the gap between two electrodes is too large, then the droplet will stop at the middle region, where the driving force is smaller than the friction force. Therefore, in order to increase the maximum driving distance of the droplet, we can either increase the applied potential on two electrodes or decrease the contact angle of the droplet.

The electrical output performances of this freestanding TENG with different number of Al foils are shown in Figure 3a–c. For the measurement of the prepared freestanding TENG, the top plate adhered by Kapton film is the movable object, while the bottom plate adhered by Al foil is fixed on some substrate, and a linear motor is applied to guide the horizontal sliding motion of the top plate. At the beginning stage, the Kapton is placed on the surface of the first Al foil. The Kapton surface is in close contact with Al foil, and the open-circuit voltage (V_{oc}) is close to zero because all of the tribo-induced charges stayed at the neutralized state. When Kapton film slides to the second Al foil, the positive charges stay at the first foil, and the output voltage from the first foil is also positive (Figure 3d, black line). Meanwhile, the output voltage from the second foil is negative (Figure 3d, blue line), which is induced by the negative charges on the Kapton film.

DOI: 10.1021/acsnano.7b08014
ACS Nano 2018, 12, 1491–1499

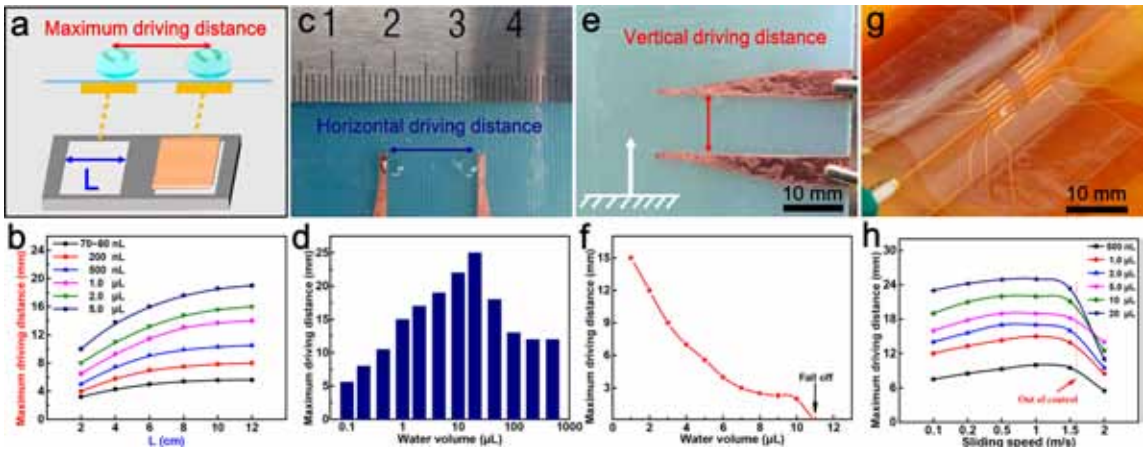

Figure 4. Performance of one droplet driven by TENG. (a) The illustration of the simple self-powered microfluidic transport system (*L*: width of the Al foil). (b) The maximum driving distance with different *L*. The minimum of droplet volume is about 70−80 nL. (c) The photograph of horizontal movement of one water droplet driven by TENG. (d) The horizontal driving distance with different droplet volume. (e) The photograph of vertical movement of a droplet. (f) The vertical driving distance with different water volume. (g) The photograph of one water droplet climbing one step driven by TENG. (h) The maximum driving distance with different sliding speeds of Kapton.

When the Kapton returned to the first Al foil, the voltage polarity on two Al foils switched, and a continuous voltage output can be achieved by repeating this sliding motion. The amplitude of voltage output increased gradually and saturated after four cycles, which indicated that the Kapton surface has a maximum charge density. The output voltage from this two electrode TENG finally increased to the maximum value about 3500 V. For the freestanding TENG with three (Figure 3b) and four electrodes (Figure 3c), the voltage performances of these two devices are shown in Figure 3e,f, respectively. It can be found that the voltage signal from the double-electrode TENG (Figure 3d) is a pick signal, while the voltage signals from the other two cases are square wave signals (Figure 3e,f). This is caused by the motion trace of the Kapton film. There is no pause for the motion of Kapton in the double-electrode TENG, while for the sample with three or four electrodes, the Kapton film needs a time interval to slide across one or two middle electrodes before it can return to the initial electrode. This time interval can generate the flat signal in the voltage measurement. We also prepared the TENG device with seven foil electrodes, and the related voltage output can be seen in Figure S3. During the sliding motion, the foil electrode on different position shows different voltage waveform, which is also due to the different time interval in the repeating motion. We have also measured short-circuit current (I_{sc}) and transferred charge from this freestanding TENG, as can be shown in Figure 3g,h. Here, the output signal from each electrode is almost the same. The I_{sc} at steady state is about 7.2 μA, and the maximum transferred charges is about 0.37 μC.

In order to study the detailed operation performance of the microtransport system, we started with the double-electrode device with only one droplet and analyzed the detailed driving capability of freestanding TENG for manipulating the droplets. The structure of this simplest microtransport system is shown in Figure 4a, where maximum driving distance is the distance of droplet driven by TENG and *L* represents the width of the Al foil (the length of the foil is fixed to be 10 cm). The maximum driving distance is the farthest motion distance of the water droplet, where the droplet can still go back to the initial position. The maximum driving distance of the water droplet with different *L* is measured, as displayed in Figure 4b. The increase of *L* results in the increase of the area of Al foil, which further increases the output voltage. Hence, with the increase of *L*, the maximum driving distance increases, and the maximum driving distance increases slowly and when *L* is >8 cm. The amplitude of voltage output increased gradually with the *L* increasing, as can be seen in Figure S4a. In this system, the minimum volume of the droplet that can be effectively manipulated is 70−80 nL. (Our injector is not able to precisely control the volume of the droplet at this scale, and we can approximately estimate the volume of the droplet is between 70 and 80 nL.) When the size of Kapton and Al area is 20 cm^2, the smallest droplets can be driven to slide a distance of 3 mm, and the repeatability of this operation is 100%. If we keep decreasing the area of Kapton film (10 cm^2), then the water droplet can still be driven by the system (driving distance ≈2 mm), but the repeatability of this actuation can not be guaranteed to be 100%. The detailed demonstration of the motion of the water droplet can be seen in Movie S1 in the Supporting Information. As the volume of water droplet decreases, the maximum driving distance decreased. Due to the tribo-electrification with the air, water droplet can naturally carry some positive charges.[25,26] With the decrease of volume, surface area of droplet decreased accordingly, which means the carried charges on the droplet are also decreased. Accordingly, the TENG may not be able to generate enough Coulomb force to move the droplet. Therefore, the minimum volume of the droplet in this microtransport system can illustrate the driving capability of the TENG device. In this experiment, the minimum volume of the droplet can reach 70−80 nL, which is about 250 times smaller than the previous study.[20] This result can demonstrate the superior capability of this microtransport system. The horizontal driving distances of the water droplet with different volumes are detailed studied and summarized, as shown in Figure 4c,d. The area of Kapton and Al used for these and later studies is 10 cm × 8 cm. The optimized volume for this microsystem is about 20−40 μL, and the maximum driving distance is about 25 mm. In order to further develop the application potential of this system, the vertical movement of the water droplet under the drive of TENG is also studied in this research. The photograph of vertical movement of one water droplet driven by TENG is shown in Figure 4e, and the

DOI: 10.1021/acsnano.7b08014
ACS Nano 2018, 12, 1491−1499

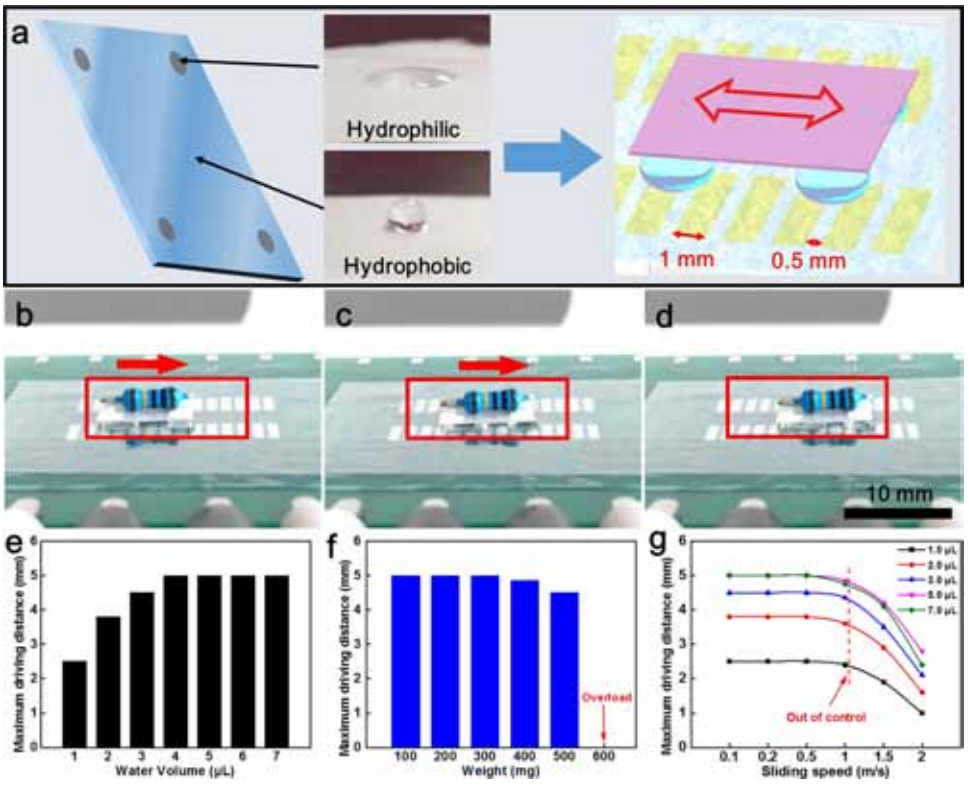

Figure 5. Structure and performance of the self-powered microfluidic transport system driving a mini vehicle. (a) Production process of the mini vehicle. By hydrophobic treatment, only four corners of the PVDF electrospinning film are hydrophilic. (b–d) The photographs of movement of the mini vehicle with a resistor driven by TENG. (e) The maximum driving distance of the mini vehicle with different water volume. (f) The maximum driving distance of the mini vehicle with different load. The mini vehicle will overload when the amount of the tiny object is more than 500 mg. (g) The maximum driving distance with different sliding speeds of Kapton. The mini vehicle will be out of control when the sliding speed is over 1.0 m/s.

experimental data can be seen in Figure 4f. The demonstration of vertical movement of one water droplet driven by TENG can be seen in Movie S2. It is important to note that the droplet is fixed on the vertical plane due to the Coulomb force induced by TENG, since Coulomb force together with the friction between droplet and FEP are greater than the gravity of droplet. However, for the water droplet larger than 10 μL, the water droplet fell off the vertical plane (Figure 4f). Figure 4g shows a photograph about the droplet climbing up one step under the drive of TENG, and the detail demonstration can be seen in Movie S2. For analyzing more detailed performances of this self-powered microfluidic transport system, we tested the effect of different sliding speeds on the maximum driving distance, as shown in Figure 4h. The optimized sliding speed is about 0.5–1.5 m/s, while the droplet will be out of control when the sliding speed over 1.5 m/s. Correspondingly, the amplitude of voltage output with different sliding speeds is shown in Figure S4b. With the increase of sliding speed, the voltage slowly decreases.

The concept of this self-powered microfluidic transport system provides a promising application of TENG as a motion-tunable actuator to drive and to control microfluidic systems. Not only a single droplet but also four droplets as a mini vehicle can be manipulated. As can be seen in Figure 5a, an actuation system based on freestanding TENG with four Al foils is established for manipulating the motion of the mini vehicle. The detail demonstration can be seen in Movie S3. In this system, with hydrophobic treatment by organic silicon resin, a PVDF pallet (6 mm × 8 mm) can be achieved (Movie S4). The four corners of the PVDF film are still hydrophilic, and thus four droplets can be attracted on these four corners. It is important to note that a hydrophobic treatment needs to be done before placing the pallet on the droplets in order to isolate the droplets from each other, otherwise they are merged together. In addition, when the tiny object is taken away from the pallet, the elliptical shape of droplets can recover only with hydrophobic PVDF surface (see Figure S5a–b). Hence, the hydrophobic treatment can also extend the service life of the mini vehicle for the system. Furthermore, this mini vehicle can carry a resistor driven by TENG, and the photographs of the motions of a mini vehicle with a resistor are shown in Figure 5b–d, respectively. The corresponding demonstration can be seen in Movie S3. In order to study the performance of mini vehicle movement, different volumes of water droplets are applied in the experiment. Figure 5e shows the maximum driving distance of mini vehicle with different volume of water droplet, where the size of the pallet is the same. In this experiment, the minimum volume of droplet can reach 1.0 μL, and the corresponding maximum driving distance is 3 mm. For the smaller droplets, the size and the weight of the pallet should also be modified, and the optimized combination can further improve the motion performance. In addition, we tested the relationship between the movement distance and the load. Figure 5f shows the maximum driving distance with different loads, where the maximum load is 500 mg. The photograph of a mini vehicle carrying a small object with 500 mg is shown in Figure S6. When the weight of tiny object is over 500 mg, the mini vehicle is overloaded and can not freely move. On the

DOI: 10.1021/acsnano.7b08014
ACS Nano 2018, 12, 1491–1499

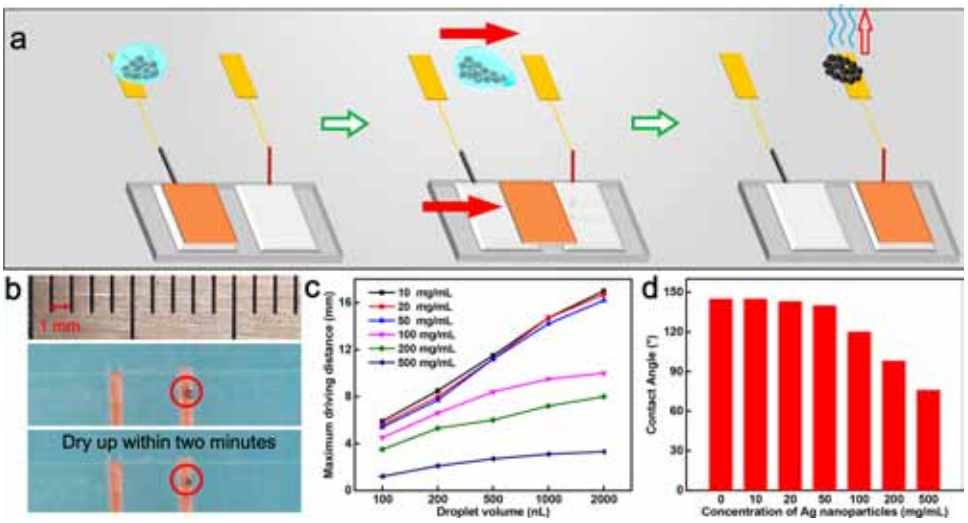

Figure 6. Structure and performance of the self-powered microfluidic transport system to carry nanoparticles. (a) Schematic diagram of the self-powered microfluidic transport system driving a droplet with nanoparticles. (b) The photograph of droplet carrying nanoparticles before and after drying up within 2 min. (c) Maximum driving distance with different droplet volume. (d) The contact angle with different concentration of Ag nanoparticles.

other hand, the sliding speed of Kapton also has an impact on the movement of the mini vehicle. The maximum driving distance with different sliding speeds of Kapton is shown in Figure 5g, where the mini vehicle is out of control with the sliding speed over 1.0 m/s. The output voltage of TENG with different sliding speed is shown in Figure S4b.

The reported mini vehicle can deliver a tiny object in millimeter scale, which is mainly decided by the size of pallet. Based on the handcraft in our lab, it is not easy to maintain the flexibility of the vehicle motion if the size of the pallet is smaller than 1 mm. Hence, we presented another strategy to deliver the tiny object with much smaller size. Figure 6a shows the schematic diagram of the self-powered microfluidic transport system driving some nanoparticles to the designated position. The nanoparticles (or other tiny objects) should be nonsoluble materials, and they are first immersed in the water droplet. Then, the droplet as well as the immersed object are driven by the electrostatic field induced by TENG, the mechanism of which is similar to that shown in Figure 2. Finally, the droplet carried the nanoparticles to the designated position, and the nanoparticles are left there after water volatilized. This strategy is suitable for the droplet with tiny volume, and thus the volatilization process of the droplet should be very quick. The demonstration can be seen in Movie S5, where Ag nanoparticles are dispersed in the water droplet. In this experiment, the volume of the droplet is about 100 nL, and the water volatilized within 2 min in room temperature (Figure 6b). In the experiment, we found that the concentration of Ag nanoparticles in the droplet had a significant effect on the droplet moving distance. Figure 6c shows the maximum driving distance with different droplet volume, where the maximum driving distance decreases drastically when the concentration of Ag nanoparticles is >100 mg/mL. However, when the concentration is <50 mg/mL, the maximum driving distance is almost constant. The main reason can be attributed to the change of contact angle for droplet with different nanoparticle concentrations. Figure 6d shows the contact angle change with different concentrations of Ag nanoparticles. It can be seen that the contact angle is maintained at between 140° and 145° at a concentration <50 mg/mL, while the contact angle decreased drastically with the concentration >100 mg/mL. The photographs of contact angle of three different concentrations of Ag nanoparticles are show in Figure S7. The contact angle of concentration of 10 mg/mL (Figure S7a) is almost equal to the contact angle of ultrapure water (inset of Figure 1e). The contact angle is about 94° and 75° when the concentration is 200 mg/mL (Figure S7b) and 500 mg/mL (Figure S7c), respectively. In spite of this, the droplets can still be driven at a contact angle of 100°. The demonstration can be seen in Movie S6, which is a specific microscopic motion of water droplets taken with a high-speed camera (video playback speed slowed 50 times.) The detailed relationship between contact angle and the sliding motion of the droplet has been intensively studied by the other researchers.[23,24] Generally speaking, the sliding motion of water droplets becomes easier with the increase of contact angles in the highly hydrophobic region. This strategy can be an alternative for establishing a self-powered microfluidic transport system, and it can also further improve the practicability of this TENG-based microfluidic technology.

CONCLUSION

In summary, a self-powered microfluidic transport system has been designed based on freestanding TENG and electrowetting technique. A mini vehicle is fabricated by using four droplets to carry a pallet, and the electrostatic field provided by freestanding TENG can generate Coulomb force to move the droplets. The freestanding TENG has been proved to have excellent capability to drive microfluid, and the minimum volume of the droplet can reach 70−80 nL. Under the drive of TENG, the tiny droplet can freely move on both horizontal and vertical planes, while it can also climb up a step, indicating the great applicability of this system. Hence, the mini vehicle can deliver some tiny objects under the drive of TENG. The maximum load for this mini vehicle is 500 mg, and the highest controllable velocity can reach 1 m/s. The sliding motions of TENG can serve as the driving power for the system, and TENG can precisely guide the step motion of microfluids. Finally, as a supplement for the transport system, another strategy for delivering some micro-object to the designated position has also been demonstrated. This TENG-based

DOI: 10.1021/acsnano.7b08014
ACS Nano 2018, 12, 1491−1499

microtransport system has self-powered capability, high efficiency, and fast response speed. Meanwhile, it can realize manual control without any detector or control circuit, which allows it to serve as the bridge for human-machine interactions. A wide variety of potential applications can be demonstrated based on this conjunct system, including inkjet printing, drug delivery, micromanipulators, and even liquid robotics.

EXPERIMENTAL SECTION

Fabrication of Freestanding TENG. The freestanding TENG designed for this experiment had two plates (a fixed one and a moveable one) to serve as motion objects. Here, the supporting substrates are employed on each plate to ensure the close contact during its motion. For the fixed plate, three different amounts of Al foils (two Al foils are used to drive a droplet movement, four Al foils are used to drive a mini vehicle, seven Al foils are used to drive a droplet to climb a step) with rectangular shape (8 cm × 10 cm) are attached on its top surface, where the foil could functionalize as both tribosurface and the output electrode. The gap between Al foils is 1 cm. The other tribo-surface is the surface of a Kapton adhesive tape (thickness ≈50 μm, 8 cm × 10 cm), which is adhered on the surface of the moveable plate. The ICP reactive-ion etching process is performed on the surface of Kapton tape, in order to achieve nanopatterned structures. The detailed parameters for the ICP treatment can be seen in the reference paper.[19]

Measurement of Freestanding TENG. The moveable plate with Kapton is driven periodically by a numerical controllable linear motor, where the two plates are kept in parallel with each other, and their inner surfaces are kept in intimate contact. The sliding speed of the Kapton is controlled by the numerical controllable linear motor. The output performance of output charge and current is measured by Keithley 6514 System Electrometer. The voltage is measured by TREK 347 System Electrometer.

Fabrication of the Microtransport System. The grid electrodes for manipulating mini vehicle are PCB, and the electrodes are connected through the wiring on the circuit board. In order to prevent breakdown phenomenon between adjacent electrodes, a layer of polytetrafluoroethylene (PTFE) tape is attached to the grid electrodes. The FEP film is hydrophobic treatment by polyether siloxane copolymer (TEGO, Degussa) and is attached on top of PTFE, and the water droplets could move smoothly on the surface of the FEP film. The PVDF electrospining film is attached on a polystyrene substrate, and then it is hydrophobic treated by polyether siloxane copolymer (TEGO, Degussa) in order to isolate the droplets from each other. For the self-powered microfluidic transport system to drive one droplet with Ag nanoparticles, the electrodes are made of Cu tape, while the Ag nanoparticles are purchased from Sigma (50 nm). The deflection angle of the pellet is recorded by a fixed high-speed camera (PHOTRON, AX200). The morphology of the surface FEP and Kapton is observed through scanning electron microscopy (SEM, Hitachi SU-8020).

The Fabrication of the PVDF Electrospining Film. The fabrication procedure of the PVDF electrospining film is based on a far-field electrospun process. The PVDF powder with an average M_w of 530,000 is dissolved into a mixture of dimethylformamide and acetone (3:7 in volume) at 12% of mass and then stirred at the temperature of 60 °C for 2 h until the solutions become homogeneous and clear. Subsequently, the solutions are filled in 20 mL plastic syringes and fed at a constant speed of 2 mL/h through a micropump. The positive node of a high voltage supply is connected to the syringe needle with a bias voltage around 10 kV. The drum with the diameter of 8 cm covering of a copper net is placed 10 cm away from the needle and connects to a negative node with a bias voltage around 2 kV. The rotation speed of 500 rpm is set for the drum to effectively collect aligned nanofibers. After continuously collecting for about 2 h, the nanofiber arrays form a film with a thickness of about 50 μm. Finally, the nanofiber film is annealed at the temperature of 60 °C for 5 h in a vacuum drying oven.

ASSOCIATED CONTENT

Supporting Information

Movie S1 (AVI) Movie S2 (AVI) Movie S3 (AVI) Movie S4 (AVI) Movie S5 (AVI) Movie S6 (AVI) The Supporting Information is available free of charge on the ACS Publications website at DOI: 10.1021/acsnano.7b08014.

Additional information and figures (PDF)
Movie S1; one droplet driven by TENG (AVI)
Movie S2; the vertical movement of a droplet driven by TENG (AVI)
Movie S3; two droplets and a mini vehicle driven by TENG (AVI)
Movie S4; the wettability of PVDF film before and after hydrophobic treatment (AVI)
Movie S5; the droplet carrying Ag nanoparticles driven by TENG (AVI)
Movie S6; microscopic motion of droplet (AVI)

AUTHOR INFORMATION

Corresponding Authors

*E-mail: chenxiangyu@binn.cas.cn.
*E-mail: mcli@ncepu.edu.cn.
*E-mail: zlwang@gatech.edu.

ORCID

Meicheng Li: 0000-0002-9756-742X
Zhong Lin Wang: 0000-0002-5530-0380

Notes

The authors declare no competing financial interest.

ACKNOWLEDGMENTS

This work is supported by the National Key R&D Project from Minister of Science and Technology (2016YFA0202704), the "thousands talents" program for pioneer researcher and his innovation team, China, NSFC Key Program (no. 21237003) and National Natural Science Foundation of China (grant nos. 51775049, 51432005, 11674215, 5151101243, 51561145021).

REFERENCES

(1) Monat, C.; Domachuk, P.; Eggleton, B. J. Integrated Optofluidics: A New River of Light. *Nat. Photonics* **2007**, *1*, 106−114.
(2) Atencia, J.; Beebe, D. J. Controlled Microfluidic Interfaces. *Nature* **2005**, *437*, 648−655.
(3) Comiskey, B.; Albert, J. D.; Yoshizawa, H.; Jacobson, J. An Electrophoretic Ink for All-Printed Reflective Electronic Displays. *Nature* **1998**, *394*, 253−255.
(4) Hayes, R. A.; Feenstra, B. J. Video-Speed Electronic Paper Based on Electrowetting. *Nature* **2003**, *425*, 383−385.
(5) Prins, M. W.; Welters, W. J. J; Weekamp, J. W. Fluid Control in Multichannel Structures by Electrocapillary Pressure. *Science* **2001**, *291*, 277−280.
(6) Moon, H.; Cho, S. K.; Garrell, R. L.; Kim, C.-J. C. Low Voltage Electrowetting-on-Dielectric. *J. Appl. Phys.* **2002**, *92*, 4080−4087.
(7) Zhong, J. W.; Zhong, Q. Z.; Fan, F. R.; Zhang, Y.; Wang, S. H.; Hu, B.; Wang, Z. L.; Zhou, J. Finger Typing Driven Triboelectric Nanogenerator and Its Use for Instantaneously Lighting up LEDs. *Nano Energy* **2013**, *2*, 491−497.
(8) Wang, X.; Yin, Y.; Yi, F.; Dai, K.; Niu, S.; Han, Y.; Zhang, Y.; You, Z. Bioinspired Stretchable Triboelectric Nanogenerator as Energy-Harvesting Skin for Self-Powered Electronics. *Nano Energy* **2017**, *39*, 429−436.
(9) Jeong, C. K.; Kim, I.; Park, K.-I.; Oh, M. H.; Paik, H.; Hwang, G.-T.; No, K.; Nam, Y. S.; Lee, K. J. Virus-Directed Design of a Flexible $BaTiO_3$ Nanogenerator. *ACS Nano* **2013**, *7*, 11016−11025.

DOI: 10.1021/acsnano.7b08014
ACS Nano 2018, 12, 1491−1499

(10) Hinchet, R.; Kim, S.-W. Wearable and Implantable Mechanical Energy Harvesters for Self-Powered Biomedical Systems. *ACS Nano* **2015**, *9*, 7742−7745.
(11) Shi, M.; Zhang, J.; Chen, H.; Han, M.; Shankaregowda, S. A.; Su, Z.; Meng, B.; Cheng, X.; Zhang, H. Self-Powered Analogue Smart Skin. *ACS Nano* **2016**, *10*, 4083−4091.
(12) Chen, X.; Iwamoto, M.; Shi, Z.; Zhang, L.; Wang, Z. L. Self-Powered Trace Memorization by Conjunction of Contact-Electrification and Ferroelectricity. *Adv. Funct. Mater.* **2015**, *25*, 739−747.
(13) Seung, W.; Gupta, M. K.; Lee, K. Y.; Shin, K.-S.; Lee, J.-H.; Kim, T. Y.; Kim, S.; Lin, J.; Kim, J. H.; Kim, S.-W. Nanopatterned Textile-Based Wearable Triboelectric Nanogenerator. *ACS Nano* **2015**, *9*, 3501−3509.
(14) Zhong, J.; Zhang, Y.; Zhong, Q.; Hu, Q.; Hu, B.; Wang, Z. L.; Zhou, J. Fiber-Based Generator for Wearable Electronics and Mobile Medication. *ACS Nano* **2014**, *8*, 6273−6280.
(15) Lee, K. Y.; Gupta, M. K.; Kim, S.-W. Transparent Flexible Stretchable Piezoelectric and Triboelectric Nanogenerators for Powering Portable Electronics. *Nano Energy* **2015**, *14*, 139−160.
(16) Niu, S.; Liu, Y.; Chen, X.; Wang, S.; Zhou, Y. S.; Lin, L.; Xie, Y.; Wang, Z. L. Theory of Freestanding Triboelectric-Layer-Based Nanogenerators. *Nano Energy* **2015**, *12*, 760−774.
(17) Chen, X.; Wu, Y.; Yu, A.; Xu, L.; Zheng, L.; Liu, Y.; Li, H.; Wang, Z. L. Self-Powered Modulation of Elastomeric Optical Grating by Using Triboelectric Nanogenerator. *Nano Energy* **2017**, *38*, 91−100.
(18) Chen, X.; Pu, X.; Jiang, T.; Yu, A.; Xu, L.; Wang, Z. L. Tunable Optical Modulator by Coupling a Triboelectric Nanogenerator and a Dielectric Elastomer. *Adv. Funct. Mater.* **2017**, *27*, 1603788.
(19) Chen, X.; Jiang, T.; Yao, Y.; Xu, L.; Zhao, Z.; Wang, Z. L. Stimulating Acrylic Elastomers by a Triboelectric Nanogenerator-Toward Self-Powered Electronic Skin and Artificial Muscle. *Adv. Funct. Mater.* **2016**, *26*, 4906−4913.
(20) Zheng, L.; Wu, Y.; Chen, X.; Yu, A.; Xu, L.; Liu, Y.; Li, H.; Wang, Z. L. Self-Powered Electrostatic Actuation Systems for Manipulating the Movement of both Microfluid and Solid Objects by Using Triboelectric Nanogenerator. *Adv. Funct. Mater.* **2017**, *27*, 1606408.
(21) Yu, Y.; Sun, H.; Orbay, H.; Chen, F.; England, C. G.; Cai, W.; Wang, X. Biocompatibility and *In Vivo* Operation of Implantable Mesoporous PVDF-Based Nanogenerators. *Nano Energy* **2016**, *27*, 275−281.
(22) Chen, X.; Wu, Y.; Shao, J.; Jiang, T.; Yu, A.; Xu, L.; Wang, Z. L. On-Skin Triboelectric Nanogenerator and Self-Powered Sensor with Ultrathin Thickness and High Stretchability. *Small* **2017**, *13*, 1702929.
(23) Miwa, M.; Nakajima, A.; Fujishima, A.; Hashimoto, K.; Watanabe, T. Effects of the Surface Roughness on Sliding Angles of Water Droplets on Superhydrophobic Surfaces. *Langmuir* **2000**, *16*, 5754−5760.
(24) Yoshimitsu, Z.; Nakajima, A.; Watanabe, T.; Hashimoto, K. Effects of Surface Structure on the Hydrophobicity and Sliding Behavior of Water Droplets. *Langmuir* **2002**, *18*, 5818−5822.
(25) Zheng, L.; Lin, Z.-H.; Cheng, G.; Wu, W.; Wen, X.; Lee, S.; Wang, Z. L. Silicon-Based Hybrid Cell for Harvesting Solar Energy and Raindrop Electrostatic Energy. *Nano Energy* **2014**, *9*, 291−300.
(26) Choi, D.; Lee, H.; Im, D. J.; Kang, I. S.; Lim, G.; Kim, D. S.; Kang, K. H. Spontaneous Electrical Charging of Droplets by Conventional Pipetting. *Sci. Rep.* **2013**, *3*, 2037.

DOI: 10.1021/acsnano.7b08014
ACS Nano 2018, 12, 1491−1499